Supp. Figure S1: X chromosome inactivation (XCI) results from 288 female ID patients. Number of female patients in each XCI ratio interval are depicted on top of each bar.

Supp. Figure S2: Pictures of patient 2. Patient 2 has a *de novo* stop variant in *DDX3X* (NM_001193417.2:c.529G>T:p.G177X). Dysmorphic features include triangular facies with arched and hairy eyebrows, hypertelorism, downslanting palpebral fissures, large dysmorphic ears, convergent strabismus, a long philtrum and micrognathism. She also has slender fingers.

Supp. Figure S3: Pictures of patient 3. Patient 3 has a *de novo* nonsynonymous variant in *SMC1A* (NM_006306.3:c.2351T>C:p.I178T). Phenotypic features are described in Supp. Table S3.

Supp. Figure S4: Pictures of patient 8. Patient 8 has a nonsynonymous *de novo* variant in *HDAC8* (NM_018486.2:c.958G>A:p.G320R). The patient does not have facial features consistent with Cornelia De Lange syndrome, instead a shortened philtrum that shows large protruding teeth.

Supp. Table S1: Sequences of primers (5' to 3') and their position in the genome

---

X-inactivation analysis primers

Primer ID	Forward primer	Reverse primer	Position start[a]	Size (bp)
AR	TCCAGAATCTGTTCCAGAGCGTGC	CTGGGACGCAACCTCTCTC	X:66765056	330
PCSK1N	ATGCGAAGACCATTCCCTCT	GTGCGTGTGATGTGAGGAGA	X:48693154	340
PGK1	TGTTCCGCATTCTGCAAGCC	TATCCTTTTGTGCAGGAACC	X:77359744	622

Mutation screening of a 3 kb region of XIST by PCR and Sanger sequencing

Primer ID	Forward primer	Reverse primer	Position	Size (bp)
XIST1	CTTTCTGGTATGTCTTTGCT	CAGAGGGGAAGGGAATCA	X:73072043	686
XIST2	CGTGGATACCTGCCTTTT	CTGCACCTTAGTCTTTCCT	X:73071403	761
XIST3	ATTTGGGGCTTGTTAGGA	GGGGACAAATAAGAGGGGA	X:73070712	807
XIST4	GGGTGAATTAGCATGGCACT	GCAAACCACAAAATCAGACTGT	X:73070274	598
XIST5	TGGGGTCGGATTTTGATTTA	TGAAGATCAGCAATGCCAAG	X:73069528	813

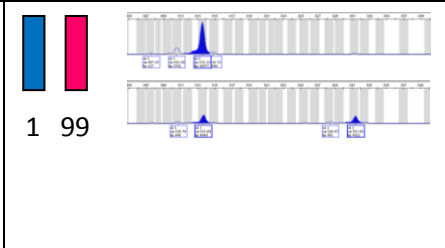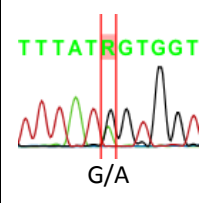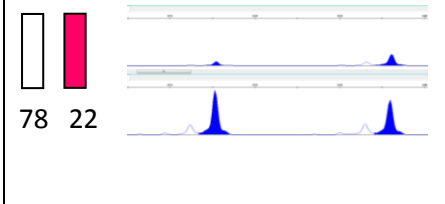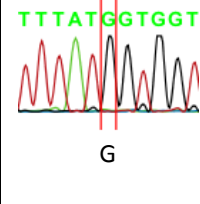*Confirmation of whole exome sequencing data by PCR and Sanger sequencing*
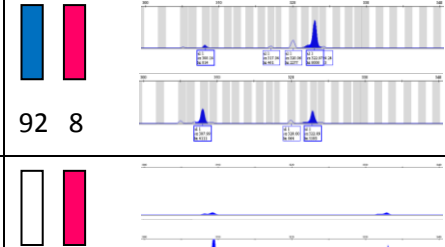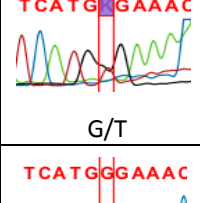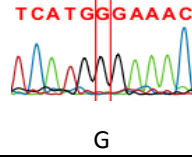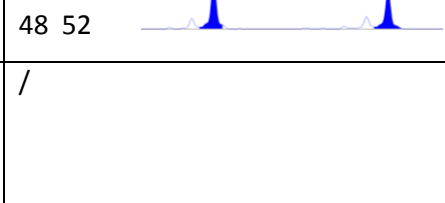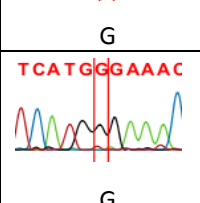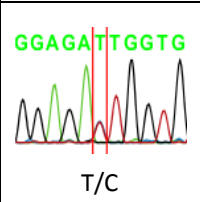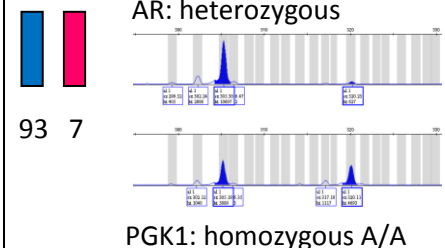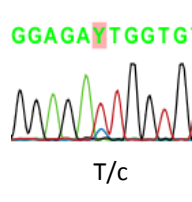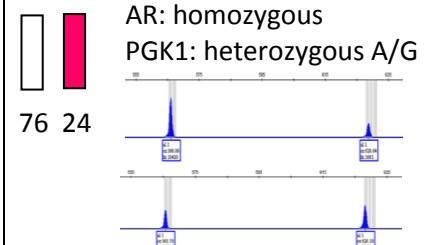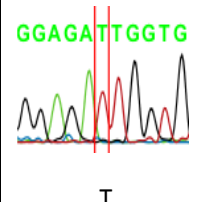
Primer ID	Forward primer	Reverse primer	Position	Size (bp)
DDX3X	CAAACAATACCCAATCTCC	TTCCTCTTTCCATCATATCC	X:41203306	325
DDX3X	GCTGTTGGTTGGTTGTTT	TTGAGCTTACCTGTTTGGG	X:41202385	230
SMC1A	CGAGAGAGGGAAATGAAAGA	AAGGCCTAGCTACATAAAC	X:53430368	383
WDR45	ACACACAATCCAAGGAGAAA	GGTATGGTAAATGGGCAG	X:48932966	302
NHS	CACAACTTAAAGCCACTGA	GAGTTGTCTCCCGCAAAA	X:17705814	243
MECP2	TCCTTTCCCGCTCTTCTC	GCCTTTTCAAACTTCGCC	X:153296274	334
MED12	ACTCATTTCTTTGTCCCC	CTCTTCTCTACTTTCGCCT	X:70342887	365
HDAC8	TCTTTCCTTACCCCCCTTC	ACTCAGCTCTTCCCCTTA	X:71681804	222
EP300	CCAACTCTAATCCACAACC	CCATATTTCCTTGTTGCATC	22:41573993	441
SYNGAP1	GGCATTCAACTCACATCT	CCCATCGTACCCTATCCA	6:33412059	346
TAF9B	GAGAGAACAAAAACAGGAC	AGCTTTACTAGAGGATGAG	X:77392266	349
TTN	GTGATACAACTGGGGAGA	GGAAAAAAGAGGAGAATGG	2:179466698	350
TTN	GTGATGTTTGTACCCTTGA	GATGAACAAAAGGATGGGA	2:179542275	405

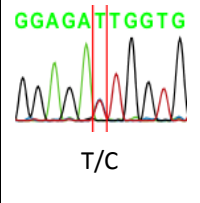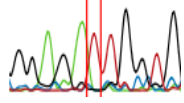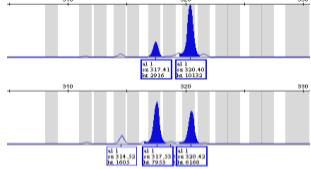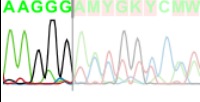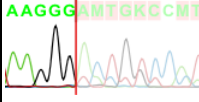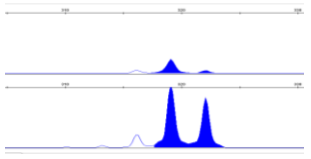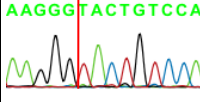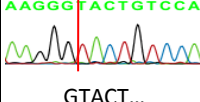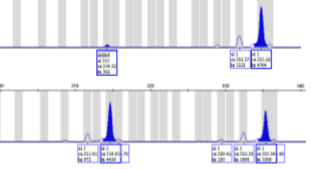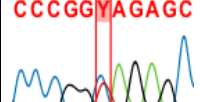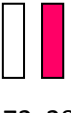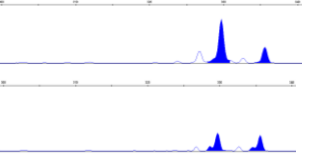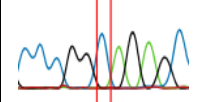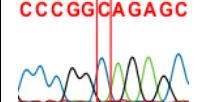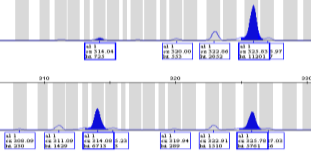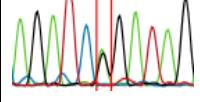*cDNA analysis by PCR and Sanger sequencing*
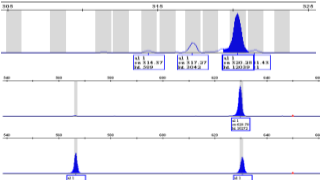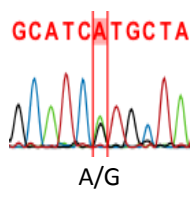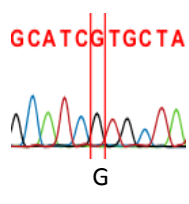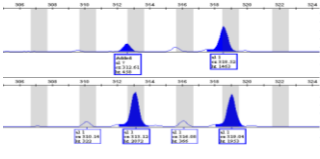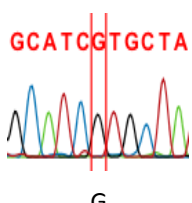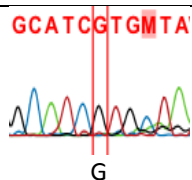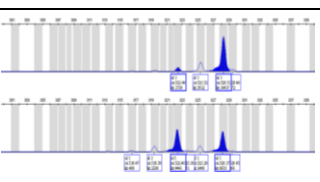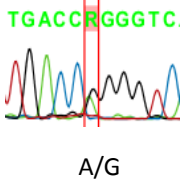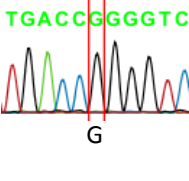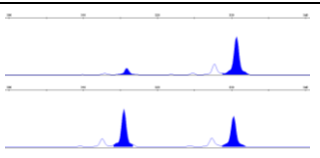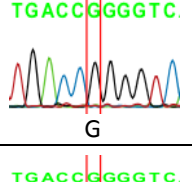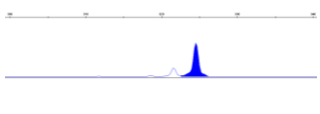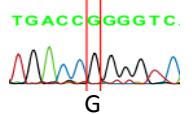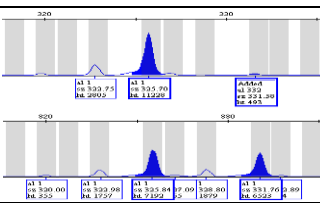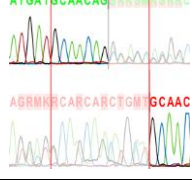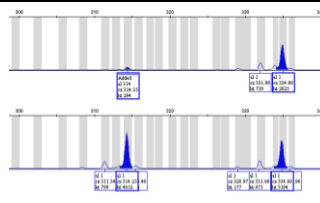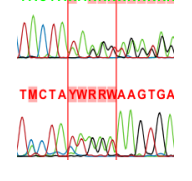
Primer ID	Forward primer	Reverse primer	Position	Size (bp)
SMC1A (cDNA)	AGAACAGACCAAGACACGA	TCTCAAACTCCAAACGCT	X:53430498	278
WDR45 (cDNA)	TACCCTTATTCGCCTCTTT	TACGCAGATGGCAATGAC	X:48932561	343
MED12 (cDNA)	GATGATGATGCTGTGGTGT	GAAAATGGGAGCACTGGG	X:70342954	204
HDAC8 (cDNA)	TGACACAATAGCTGGGGA	GATGTAGTTGAGGATTTGTTGG	X:71571587	310
DDX3X (cDNA)	CAAAACCACTCCCACCAA	CCATACCTTCCATTTTCCTTCA	X:41201873	373

---
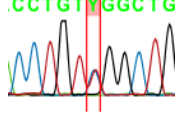
[a]positions based on Hg19

Supp. Table S2: Summary of the XCI, Sanger sequencing confirmation and expression analysis data of the variants detected by WES in patients 1-10

Sample	XCI pattern (% inactive)	GOI + variant	gDNA (Sanger confirmation)	cDNA (expression analysis)
Patient 1	1 99	*DDX3X* NM_001193417.2 :c.856G>A:p.G286S	TTTAT**R**GTGGT G/A	/
Mother 1	78 22		TTTAT**G**GTGGT G	/
Patient 2	92 8	*DDX3X* NM_001193417.2 :c.529G>T:p.G177X	TCATG**K**GAAAC G/T	TCATG**G**GAAAC G
Mother 2	48 52		TCATG**G**GAAAC G	/
Father 2	/		TCATG**G**GAAAC G	/
Patient 3	93 7 AR: heterozygous PGK1: homozygous A/A	*SMC1A* NM_006306.3:c.2351T>C:p.I784T	GGAGA**T**TGGTG T/C	GGAGA**Y**TGGTG T/c
Mother 3	76 24 AR: homozygous PGK1: heterozygous A/G		GGAGA**T**TGGTG T	/

Sample	XCI pattern (% inactive)		GOI + variant	gDNA (Sanger confirmation)	cDNA (expression analysis)
Father 3	/			GGAGA TTGGTG T	/
Patient 4	7 93		*WDR45* NM_001029896.1 :c.777delT:p.T260 Lfs*27	AAGGG AMYGKYCMW GTACT… GACTG…	AAGGG AMTGKCCMT G tact… GACTG…
Mother 4	81 19			AAGGG TACTGTCCA GTACT…	/
Father 4				AAGGG TACTGTCCA GTACT…	/
Patient 5	5 95		*NHS* NM_001136024.3 :c.163C>T:p.Q55X	CCCGG YAGAGC C/T	/
Mother 5	72 28			CCCGG CAGAGC C	/
Father 5				CCCGG CAGAGC C	/
Patient 6	6 94		*MECP2* NM_004992.3:c.8 80C>T:p.R294X	AGATC RGATAG A/G	/

Sample	XCI pattern (% inactive)		GOI + variant	gDNA (Sanger confirmation)	cDNA (expression analysis)
Patient 7	2 98	AR: homozygous PGK1: heterozygous G/A	*MED12* NM_005120.2:c.1562G>A:p.R521H	GCATCATGCTA A/G	GCATCGTGCTA G
Mother 7	21 79	AR: heterozygous PGK1: homozygous A/A		GCATCGTGCTA G	/
Father 7	/			GCATCGTGMTA G	/
Patient 8	7 93		*HDAC8* NM_018486.2:c.958G>A:p.G320R	TGACCRGGGTC. A/G	TGACCGGGGTC G
Mother 8	87 13			TGACCGGGGTC. G	/
Father 8				TGACCGGGGTC. G	/
Patient 9	4 96		*EP300* NM_001429.3:c.6567_6578del:p.2189_2193del		/
Patient 10	7 93		*TAF9B* NG_012570.1:g.7766_7770delinsAA		/

Sample	XCI pattern (% inactive)	GOI + variant	gDNA (Sanger confirmation)	cDNA (expression analysis)
		SYNGAP1 NM_006772.2:c.3494C>T:p.S1165L	CCTGTYGGCTG C/T	/

The bars depicted in the XCI pattern column represent the two X chromosomes. The percentage of inactivity is written under each X chromosome bar. The X chromosome that is inherited from the mother is depicted in red and the X chromosome that is inherited from the father is depicted in blue. This data is based on the *AR* and/or *PGK1* XCI assays. Electropherograms were obtained via the *AR* assay unless otherwise specified. GOI: gene of interest; /: unavailable.

Supp. Table S3: Comparison of clinical manifestations in three patients with identical (NM_006306.3:c.2351T>C:p.I784T) *SMC1A* variants

[Limongelli et al., 2010]	[Gervasini et al., 2013]	Patient 3 of this study
Intrauterine growth restriction (from 3rd month of pregnancy)	Growth delay in prenatal stage	Intrauterine growth restriction (from 33 weeks of pregnancy)
At 6 years weight, height and head circumference <3rd centile	Weight, height and head circumference 50th–95th centile	At 10 months weight, height and head circumference <3rd centile At 7 years, microcephaly and weight <<3rd centile
Frequent respiratory infections		Not reported
Severe gross motor delay (wheelchair at 4 years) Absent speech	Milestones in motor development delayed Absent speech	Severe gross motor delay: dystonic-hypotonic infantile cerebral palsy Hypertonia (since birth) Absent speech
Hypertrophic cardiomyopathy	Not reported	Atrial septal defect (fossa oval) Pulmonary stenosis Mild aortic coarctation
Synophrys	Arched eyebrows	Synophrys Hirsutism (from birth)
Downslanting palpebral fissures		Short palpebral fissures
Long curly eyelashes		Long eyelashes
Thin vermilion (upper lip)	Thin vermillion (upper lip)	Thin lips
Hand and feet length <3rd centile		Hallux valgus (bilateral) Feet with talus valgus reducible Dysplastic nails (some) Fifth finger clinodactyly
Ptosis	Cleft palate Neurosensory hearing loss Astigmatism Corneal ulcers Facial dysmorphism (like CdLS) Needed assisted feeding	Gastroesophageal reflux High arched palate Mild retrognatia Hearing loss (50-60%) Precocious pubarche Cerebral NMR: no findings

Patient at 6 years

Patient at 12 months

Patient at 8 years and 7 months

Supp. Table S4: Overview of the known *WDR45* mutations and summary of the reported XCI data

	Publication	gDNA/cDNA	Protein level	XCI data
		Reported male patients		
1	[Haack et al., 2012]	c.228_229del	p.Glu76Aspfs*38	/
2	[Haack et al., 2012]	c.19dup	p.Arg7Profs*64	/
3	[Haack et al., 2012]	c.1025_1034delinsACATATTT	p.Gly342Aspfs*12	/
4	[Abidi et al., 2015]	chrX:g.(48 802 381_48 809 279)_(48 829 265_48 854 335)del	Deletion of WDR45 (and CCDC120 and PRAF2)	/
		Reported female patients		
5	[Haack et al., 2012]	c.1007_1008del	p.Tyr336Cysfs*5 (reported in 2 different individuals)	random in 2/12 >75:25 in 6/12 >90:10 in 4/12
6	[Haack et al., 2012]	c.38G>C	p.Arg13Pro *predicted to cause skipping of exon 3 and an alternate start methionine at position 25	
7	[Haack et al., 2012]	c.-1_5del	p.Met1?	
8	[Haack et al., 2012]	c.293T>C	p.Leu98Pro	
9	[Haack et al., 2012]	c.476del	p.Leu159Argfs*2	
10	[Haack et al., 2012]	c.19C>T	p.Arg7X	
11	[Haack et al., 2012]	c.56-1G>A	Splicing defect	
12	[Haack et al., 2012]	c.700C>T	p.Arg234X	
13	[Haack et al., 2012]	c.400C>T	p.Arg134X	
14	[Haack et al., 2012]	c.405_409del	p.Lys135Asnfs*2	
15	[Haack et al., 2012]	c.359dup	p.Lys121Glufs*18	
16	[Haack et al., 2012]	c.830+1G>A	Splicing defect	
17	[Haack et al., 2012]	c.235+1G>A	Splicing defect	
18	[Haack et al., 2012]	c.694_703del	p.Leu232Alafs*53	
19	[Haack et al., 2012]	c.183C>A	p.Asn61Lys	
20	[Haack et al., 2012]	c.55+1G>C	Splicing defect	
21	[Saitsu et al., 2013]	c.439+1G>T	p.[Gly147Val; Val147_Leu148ins8]	NI
22	[Saitsu et al., 2013]	c.516G>C	p.Asp174Valfs*29	98:2
23	[Saitsu et al., 2013]	c.437dupA	p.Leu148Alafs*3	78:22
24	[Saitsu et al., 2013]	c.637C>T	p.Gln213X	85:15
25	[Saitsu et al., 2013]	c.1033_1034dupAA	p.Asn345Lysfs*67	97:3
26	[Hayflick et al., 2013]	c.830 + 2T>C	Splicing defect	/
27	[Hayflick et al., 2013]	c.1A>G	Start codon abolished	/
28	[Hayflick et al., 2013]	c.186delT	p.Leu63Trp fs*19	/

	Publication	gDNA/cDNA	Protein level	XCI data
29	[Verhoeven et al., 2014]	c.662_663del	p.Phe221X	/
30	[Verhoeven et al., 2014]	c.752_754del	p.Ser251del	/
31	[Verhoeven et al., 2014]	c.1030del	p.Cys344fs	/
32	[Rathore et al., 2014]	c.342-2A>C	Splicing defect	/
33	[Ichinose et al., 2014]	c.519+1_519+3del	Splicing defect	/
34	[Ozawa et al., 2014]	c.322del	p.Ser108Leufs*10	/
35	[Okamoto et al., 2014]	c.C868T	p.Gln290X	96:4
36	[Van Goethem et al., 2014]	c.488del C	p.Pro163Argfs*34	/
37	[Tschentscher et al., 2015]	c.626C > A	p.Ala209Asp	/
38	[Nishioka et al., 2015]	c.969_970insT	p.Val324CysfsX18	/
39	[Nishioka et al., 2015]	c.587_588delTA	p.Ile196SerfsX26 (reported in 2 different individuals)	/
40	[Nishioka et al., 2015]	c.414_419delGTTGA	p.Glu138_Phe139del	/
41	[Nishioka et al., 2015]	c.628T>C	p.Ser210Pro	/
42	[Ryu et al., 2015]	c.345-1G>A	Splicing defect (r.345_439del)	/
43	[Long et al., 2015]	c.251A.G	p.Asp84Gly	/
44	[Takano et al., 2016]	c. 831-1G>C	Splicing defect	/
45	[Ohba et al., 2014]	c.830+1G>A	p.Leu278X (also reported by Haack et al. 2012)	/
46	[Hamdan et al., 2014]	c.C19T	p.Arg7X (also reported by Haack et al. 2012)	/
47	[Nishioka et al., 2015]	c.400C>T	p.Arg134X (also reported by Haack et al. 2012)	/
48	[Nishioka et al., 2015]	c.293T>C	p.Leu98Pro (also reported by Haack et al. 2012)	/
49	[Khalifa and Naffaa 2015]	c.587-588del	p.196fs * + 3 missense variants in POLR3A (also reported in Nishioka et al. 2015)	/
50	[Gilissen et al., 2014]	c.1030del	p.Cys344Alafs*67 (also reported by Verhoeven et al. 2014)	/

NI: non-informative; /: not reported. Variants 1-44 are unique and variants 45-50 were reported previously.

Supp. Table S5: *MED12* mutations in female carriers

Publication	*MED12* variant	ID phenotype female carriers	XCI data (skewing >90%)
[Tzschach et al., 2015]	p.Arg815Gln	Carrier mother had learning difficulties	/
[Lesca et al., 2013]	p.Ser1967GlnfsX84	Variable cognitive impairment 1 severely affected female	1/6 female carriers skew 0/7 female non-carriers skew
[Callier et al., 2013]	p.Arg1295His	Carrier mother had mild ID	No XCI data
[Vulto-van Silfhout et al., 2013]	p.Arg1148His	/	1/1 Carrier mother skews Xi to affected son
[Vulto-van Silfhout et al., 2013]	p.Ser1165Pro	/	1/1 Carrier mother skews Xi to affected son
[Vulto-van Silfhout et al., 2013]	p.His1729Asn	/	/
[Rump et al., 2011]	p.Gly958Glu	1 mother mild learning problems (also in non-carrier sister)	/
[Lyons et al., 2009]	p.Arg961Trp	/	/
[Graham, Jr. et al., 2008]	P.Arg961Trp	/	/
[Schwartz et al., 2007]	p.Asp1007Ser	Carriers unaffected	0/4 female carriers skew 0/4 female non-carriers skew
[Risheg et al., 2007]	p.Arg961Trp	/	4/9 female carriers skew 0/4 female non-carriers skew

/: not reported or investigated.

Supp. Table S6: Overview of the reported *HDAC8* variants, their residual enzyme activity, phenotype severity and summary of reported XCI data

Residual activity enzyme compared to wild-type	Reference	Variant	Phenotype	XCI data
(0)	[Deardorff et al., 2012]	c.490C>T; p.R164X	Female: severe	
0%	[Deardorff et al., 2012]	c.539A>G; p.H180R	Female: moderate	Skewing with expression of the p.H180R mutant allele
10–50%	[Deardorff et al., 2012]	c.932C>T; p.T311M	Female: mild-severe	
10–50%	[Deardorff et al., 2012]	c.958G>A; p.G320R	Male: severe	
>50%	[Deardorff et al., 2012]	c.1001A>G; p.H334R	Female (*de novo*): severe Familial: mild-Severe in females, severe in male	Unaffected mother inactivates mutant allele.
0%	[Kaiser et al., 2014] [Ansari et al., 2014]	c.910G>A; p.G304R	Female: moderate	26 heterozygous females were tested for skewing: 20/26 skewed >95:5, 2/26 skewed >80:20, 1/26 had random XCI and 3/26 were non-informative. Interestingly the 3 samples that were not skewed >95:5 were from girls aged <4 years, which supports the theory that selection against the mutant allele in blood does not occur at an early embryonic stage.
0%	[Kaiser et al., 2014] [Ansari et al., 2014]	c.211C>T; p.H71Y	Female: mild	
0%	[Kaiser et al., 2014]	c.717_719del p.ΔK239-Y240N	Female: mild	
(0)	[Kaiser et al., 2014]	c.706C>T; p.Q236X	Female: mild	
(0)	[Kaiser et al., 2014]	c.881G>A; p.W294X	Female: severe	
<10%	[Kaiser et al., 2014]	c.350G>A; p.G117E	Female: moderate	
<10%	[Kaiser et al., 2014]	c.458G>T; p.C153F	Female: moderate	
10–50%	[Kaiser et al., 2014]	c.56T>G; p.I19S	Male: severe	
10–50%	[Kaiser et al., 2014] [Ansari et al., 2014]	c.562G>A; p.A188T	Female: mild-moderate	
10–50%	[Kaiser et al., 2014]	c.698A>G; p.D233G	Male: mild	
10–50%	[Kaiser et al., 2014]	c.709G>T; p.D237Y	Female: moderate	
10–50%	[Kaiser et al., 2014]	c.728T>A; p.I243N	Male: severe	
>50%	[Kaiser et al., 2014]	c.272C>T; p.P91L	Male: mild	
/	[Kaiser et al., 2014]	c.125A>C; p.H42P	Male: severe	
/	[Kaiser et al., 2014]	c.1006-2A>G	Female: mild	
/	[Harakalova et al., 2012]	c.164+5G>A (exon2 skipping)	7 females in family: learning difficulties and facial characteristics, males more severely affected	Affected female carriers showed extreme skewing in lymphocytes in which the mutated X-chromosome was completely inactivated.
/	[Feng et al., 2015]	c.587 A>T; p.M196K	Female: CdLS for ocular anomalies	
Deletions and duplications reported in *HDAC8*				
(0)	[Kaiser et al., 2014]	deletion, chrX:71746981-72258405 (hg19)		/
(0)	[Kaiser et al., 2014]	1827nt exon 11 deletion, chrX:71,549,304-71,551,130 (hg19)		Female: moderate
(0)	[Kaiser et al., 2014]	deletion, chrX:71,549,304-71,551,130 (hg19)		Male: severe
(0)	[Kaiser et al., 2014]	deletion, chrX:71570090-71755449 (hg19) p.Asp147Glufs*17		Female: moderate
(0)	[Kaiser et al., 2014]	deletion chrX:71681853-72434328 by exome, chrX:71632632-72449647 by array, (hg19)		Female: mild
(0)	[Kaiser et al., 2014]	deletion, chrX:71792872-71887236 (hg19)		Female: moderate
(0)	[Kaiser et al., 2014]	deletion, chrX:71,732,033-71,951,158 (hg19)		Female: mild
(0)	[Kaiser et al., 2014]	duplication chrX:71,591,275-71,712,275 (hg19) p.Phe336Leufs*1		Female: moderate

All patients had features typical of CdLS or an overlapping phenotype unless otherwise mentioned (Adapted from [Kaiser et al., 2014]).

Supp. Table S7: *De novo SYNGAP1* **variants reported in individuals with ID**

Reference	Gender	gDNA/cDNA change	Protein level
[Parker et al., 2015]	Female	chr6 g.33406569 CTGTATG>CTG	p.LYE517-519LX
[Parker et al., 2015]	Female	chr6 g.33400583G>A	p.R170Q
[Parker et al., 2015]	Female	chr6 g.33411111C>T	p.Q928X
[Parker et al., 2015]	Female	chr6 g.33411093C>T	p.R922X
[Parker et al., 2015]	Male	chr6 g.33400498 AAACGAACGAA> AAACGAA	p.KRTK142-145KRX
[Parker et al., 2015]	Female	chr6 g.33411102CT>C	p.L925X
[Parker et al., 2015]	Female	Deletion chr6:33201710- 33595089	multi-gene deletion; *SYNGAP1* plus 18 others
[Parker et al., 2015]	Female	chr6 g.33411606C>T	p.Q1079X
[Parker et al., 2015]	Male	chr6 g.33405662T>C	p.L327P
[Parker et al., 2015]	Male	chr6 g.33405662T>C	p.L327P
[Redin et al., 2014]	Male	chr6:g.33414346G>A; c.3583-6G>A;	p.V1195Afs*27
[Berryer et al., 2013]	Female	c.283dupC	p.H95PfsX5 (inherited from mosaic father)
[Berryer et al., 2013]	Male	c.1084T>C	p.W362R
[Berryer et al., 2013]	Female	c.1685C>T	p.P562L
[Berryer et al., 2013]	Male	c.2212_2213del	p.S738X
[Berryer et al., 2013]	Female	c.2184de	p.N729TfsX31
[Carvill et al., 2013]	Female	/	p.W267X
[Carvill et al., 2013]	Male	/	p.Q702X
[Carvill et al., 2013]	Male	/	K108Vfs*25
[Carvill et al., 2013]	Male	c.389-2A>T	p.? Splicing
[Carvill et al., 2013]	Female	NR	p.R143X
[Writzl and Knegt 2013]	Male	Deletion Chr6:33356364–33406339	multi-gene deletion; *SYNGAP1* plus 3 others
[de Ligt et al., 2012]	Male	Chr6(GRCh37):g.33402928G>A ; c.510-1G>A	p.? Exon skipping
[Rauch et al., 2012]	Female	Chromosome 6: g.33410958_33410959insT	p.T878Dfs*60
[Rauch et al., 2012]	Male	Chromosome 6: g.33405934_33405935delAA	p.K418Rfs*54
[Hamdan et al., 2011]	Female	c.2677delC	p.Q893Rfs
[Hamdan et al., 2011]	Male	c.321_324delGAAG	p.K108Vfs
[Hamdan et al., 2011]	Male	c.2294+1G>A	p.? Splicing
[Klitten et al., 2011]	Male	Balanced translocation: t(6;22)(p21.32;q11.21)	Breakpoint in *SYNGAP1*
[Zollino et al., 2011]	Female	300-kb deletion chr6p21.3 (33.4-33.7 Mb from telomere)	multi-gene deletion; *SYNGAP1* plus 6 others
[Krepischi et al., 2010]	Male	Deletion chr6:33273955–34086729	multi-gene deletion; *SYNGAP1* plus 18 others
[Pinto et al., 2010]	Female	Deletion chr6: 33399849- 33512042	multi-gene deletion; *SYNGAP1* plus 4 others
[Vissers et al., 2010]	Female	c.998_999del	p.V333AfsX
[Hamdan et al., 2009]	Female	C.412A→T	p.K138X
[Hamdan et al., 2009]	Female	c.1735C→T	p.R579X
[Hamdan et al., 2009]	Female	c.2438delT	p.L813RfsX22

/:not reported.

SUPP. DISCUSSION

Exome sequencing of 19 female patients with a syndromic form of ID and >90% skewing revealed variants in ten ID genes that could play a role in their clinical features. Of these, eight were located on the X chromosome. We have firm evidence that six X-linked and both autosomal variants are responsible for their phenotypes, while the evidence is less strong for the remaining two X-linked variants. Interestingly, at least six variants could be demonstrated to be *de novo* events.

Variants that likely cause XLID and skewing

DDX3X variants in patient 1 and patient 2

Recently mutations in *DDX3X* (MIM# 300160) have been identified as a common cause of ID (MIM# 300958) in female patients, in whom they are predicted to be responsible for 1-3% of unexplained ID [Snijders Blok et al., 2015]. This group further demonstrated that the *DDX3X* gene is in the top 2% of intolerant genes, meaning that normal variation in *DDX3X* is extremely rare.

To date, 35 unique deleterious *de novo* mutations in *DDX3X* have been identified in female patients with ID. Three male ID patients harboring inherited missense variants were also reported [Snijders Blok et al., 2015]. Besides ID, other clinical features reported were hypotonia, movement disorders, behavioral problems, corpus callosum hypoplasia, and epilepsy. In our cohort of 19 female patients with ID and skewing of X-inactivation we identified novel variants in *DDX3X* in 2 patients. The first patient (patient 1) carries a nonsynonymous variant (p.G286S). Similar to other patients, she also had ID and ataxic gait. This variant likely occurred *de novo* as it was not present in the mother and the father was reported to be healthy. It was located in the helicase ATP-binding domain similar to other pathogenic missense variants described in the literature [Snijders Blok et al., 2015]. The second patient (patient 2) has a *de novo* stop variant (p.G177X). She presented with hypotonia and ID, which is in line with other reported females with mutations in this gene. At cDNA level only the reference G-allele was present despite escape of X-inactivation. This may point to nonsense-mediated mRNA decay of the mutant T-allele. Haploinsufficiency of *DDX3X* was proposed by Snijders Blok and colleagues as the pathological mechanism behind ID in female patients. Interestingly, 7/15 females reported by this group had almost complete skewing of X-inactivation (>95%) which is higher than would be expected by chance

[Snijders Blok et al., 2015]. In 1/2 carrier mothers tested, extreme skewing was observed as well. This data shows that mutations in *DDX3X* likely contribute to skewing, as has been observed for other escape genes in the past [Lederer et al., 2012]. Overall, our data suggests that mutation of the escape gene *DDX3X* causes ID in female patients and can contribute to skewing of X-inactivation as well. However, the way that this is achieved remains to be identified.

SMC1A variant in patient 3

Mutations in *SMC1A* (MIM# 300040) are reported to be responsible for 5% of Cornelia de Lange syndrome (CdLS; MIM# 300590) although often with a milder presentation and without major structural anomalies. CdLS is characterized by facial dysmorphia, upper extremity malformations, hirsutism, cardiac defects, growth and cognitive retardation, gastrointestinal abnormalities and other systemic involvement. *SMC1A* partially escapes X-inactivation with 15-30% of the allele on the inactive X chromosome still being expressed [Carrel and Willard 2005]. This is corroborated by a 50% higher expression level of *SMC1A* in healthy females than in healthy males [Parenti et al., 2014]. Interestingly, SMC1A protein is expressed at similar levels in healthy females and females with *SMC1A* mutations suggesting a dominant negative effect of *SMC1A* mutations [Parenti et al., 2014]. In patient 3 we detected a nonsynonymous *de novo* variant (p.I784T) in *SMC1A*. All three patients with the same mutation had skewed X-inactivation and very similar clinical features (Supp. Table S3). . Variant *SMC1A* allelic expression was roughly 50% lower than wild type allele expression in all 6 patients tested by Parenti and colleagues, including the two patients with identical *SMC1A* variants as found in patient 3. cDNA analysis of patient 3 also indicates that the wild-type allele is preferentially expressed (Supp. Table S2). This finding suggests that the p.I784T variant-accounts for preferential skewing of X-inactivation. On the other hand, 3/7 patients studied by Parenti and colleagues had random XCI despite preferential expression of the wild-type allele. Altogether, we believe that the *SMC1A* variant-is responsible for the mild CdLS phenotype observed in patient 3 as well as for skewing of X-inactivation.

WDR45 variant in patient 4

De novo mutations in *WDR45* (MIM# 300526) cause a distinct phenotype referred to as beta-propeller protein-associated neurodegeneration (MIM# 300894), which includes early-onset global developmental delay and neurological deterioration [Haack et al., 2012]. *WDR45* is located on the X chromosome and germline mutations exclusively affect females although one male was reported with a 19.9 kb deletion in Xp11.23 containing *WDR45* [Abidi et al.,

2015]. *WDR45* was reported not to escape X-inactivation [Carrel and Willard 2005]. So far, 44 different variants in *WDR45* have been described (Supp. Table S4). Of the 17 females tested for skewing in peripheral blood, 7/17 had XCI patterns above 90:10 (Supp. Table S4). In patient 4, a novel *de novo* frameshift variant (p.T260Lfs*27) was detected in *WDR45*. At cDNA level, taking into account that this frameshift resulted in nonsense-mediated mRNA decay of the mutant transcript, the variant allele was shown to be almost exclusively used in our female patient. In lymphoblastoid cell lines derived from the females described in the literature, 4/5 subjects also exclusively expressed the mutant transcripts [Saitsu et al., 2013]. This observation is in contradiction to other X-linked mutations where skewing of X-inactivation occured against the mutant X chromosome, leading to a milder phenotype in the affected female. However, care must be taken since cell line data might not be representative for the *in vivo* situation and the XCI pattern in the brain remains undetermined. This *WDR45* variant could be a good example of one "hit" in a non-escape gene causing both ID and skewing in a female patient. However, the involvement of *WDR45* mutations in skewing remains to be studied.

Variants that likely cause XLID and not skewing

NHS variant in patient 5

Mutations in *NHS* (MIM# 300457) are known to cause Nance-Horan syndrome (MIM# 302350), which is characterized by congenital cataracts, dental anomalies, dysmorphic features, and, in some cases, ID [Burdon et al., 2003]. Patient 5 has a *de novo* stop variant (p.Q55X) in *NHS*. To date 29 pathogenic mutations in the *NHS* gene have been reported [Hong et al., 2014; Li et al., 2015] and although both genders are affected, manifestations in heterozygous carrier females have been less severe than in affected hemizygous males [Walpole et al., 1990]. . Nance-Horan syndrome patients have high phenotypic heterogeneity and no obvious genotype-phenotype correlations have been found [Florijn et al., 2006; Tug et al., 2013]. To our knowledge, this is the first report of a variant in *NHS* to cause ID in a female patient. *NHS* partially escapes X-inactivation. X-inactivation data has not been reported previously and therefore, we do not know if carrier females tend to skew against mutations in *NHS*. However, we can speculate that in this patient the *NHS* variant may be located on the active X chromosome and can therefore account for the more pronounced

phenotype. To conclude, this is the first report of a *de novo NHS* variant manifesting in a female patient causing ID, possibly due to unfavorable skewing of X-inactivation.

MECP2 variant (rs61751362) in patient 6

Mutations and rearrangements in *MECP2* (MIM# 300005) are a major cause of neurodevelopmental disorders, including Rett syndrome (MIM# 312750) in females. In patient 6, we detected the polymorphic stop variant (, p.R294X; rs61751362) in *MECP2*. This variant has been reported 216 times in RettBASE [Christodoulou et al., 2003]. It is responsible for Rett syndrome in female carriers although it generally causes less growth and nutritional problems and allows for a better preserved mobility in girls [Lundvall et al., 2006]. Patient 6 had severe ID, spastic quadriplegia, microcephaly and motor regression. We hypothesize that the variant may be located on the active X chromosome in patient 6 and thereby cause her severe phenotype. We then also expect, but were unable to identify, a second mutation responsible for skewing in this patient. On the other hand if the variant is located on the inactive X it may contribute to skewing in blood lymphocytes, as an increased frequency of preferential X-inactivation has been described previously in patients with this variant [Colvin et al., 2004]. With the threshold for skewing set at >75:25, 4/8 female patients tested had skewed XCI patterns in blood [Colvin et al., 2004]. This example clearly shows the severe difficulty to attribute causality to X-linked variants in female patients.

<u>Variants that likely cause skewing and possibly ID</u>

MED12 variant in patient 7

Mutations in *MED12* (MIM# 300188) have been reported to cause Lujan-Fryns syndrome (MIM# 309520), X-linked Ohdo syndrome (Maat–Kievit–Brunner type; MIM# 300895), and Opitz-Kaveggia syndrome (MIM# 305450) in males [Graham, Jr. and Schwartz 2013]. Interestingly all of these syndromes are characterized by ID among other features. Carrier females are usually unaffected although learning difficulties and mild ID in carrier mothers have been reported (Supp. Table S5). In patient 7, we detected a novel *de novo* missense variant (p.R521H) in *MED12*. At cDNA level only the wild-type allele was identified showing that the variant is located on the inactive X chromosome (Supp. Table S2). Since *MED12* does not escape X-inactivation we hypothesize that it is very likely responsible for skewing in blood lymphocytes in this patient. Skewing was observed in 7/21 (30%) female carriers described in the literature while 0/15 non-carrier family members skewed (Supp.

Table S5). These data strongly suggest that *MED12* mutations can lead to preferential X-inactivation in blood. However, the mechanism behind this phenomenon is ambiguous since identical *MED12* mutations have been reported to result in large differences in X-inactivation ratios [Lesca et al., 2013; Risheg et al., 2007]. This observation could mean that the X-inactivation pattern observed in blood does not necessarily correlate with that in brain and that the *MED12* variant detected in patient 7 could therefore be responsible for her ID phenotype despite preferential inactivation of the mutated allele in blood cells. Nevertheless it is more likely that the *MED12* variant of patient 7 is only responsible for skewing.

HDAC8 variant in patient 8

Like mutations in other genes of the cohensin complex, mutations in *HDAC8* (MIM# 300269) cause CdLS or CdLS-like phenotypes (MIM# 300882). So far, 22 different mutations, and 8 intragenic insertions/deletions in *HDAC8* have been reported (Supp. Table S6). All missense mutations have led to reduced or abolished activity of the enzyme [Boyle et al., 2015; Kaiser et al., 2014]. Hemizygous males are generally more severely affected than heterozygous females. Furthermore, *HDAC8* mutations in females are associated with severe skewing. Kaiser and his team reported skewing in 20/23 female patients for whom DNA from peripheral blood or cell lines was available. A further two patients had XCI patterns >80% and only one had random XCI (<80%). Interestingly, the mutant X chromosome was preferentially inactivated in 9/13 female patients, as was tested by analysing the allele expressed at cDNA level. Conversely, in 4/13 patients the mutation was located on the active X chromosome [Kaiser et al., 2014]. It is unknown whether *HDAC8* escapes X-inactivation or if XCI patterns of *HDAC8* in blood are similar in other tissues. In patient 8, we observed a nonsynonymous variant (p.G320R) in *HDAC8* located on her preferentially inactivated X chromosome. Interestingly, this exact variant was reported previously in a more severely affected male patient [Deardorff et al., 2012]. Both this male patient and our female patient had ID and growth delay. However, unlike the male patient, patient 8 does not have facial features present in classical CdLS, except for synophrys and micrognathism. Other features in common with patients bearing mutations in this gene include postnatal growth retardation, gastroesophageal reflux and hirsutism. So far, two familial *HDAC8* mutations have been described in whom both males and females are affected [Deardorff et al., 2012; Harakalova et al., 2012]. In both families, preferential X-inactivation occurred against the *HDAC8* mutated allele. Phenotypes in female carriers ranged from unaffected to severely affected. Consequently, the clinical features of patients 8 could be attributed to the *de novo HDAC8*

variant. On the other hand, we believe that it is more likely that the *HDAC8* variant is only responsible for skewing in this female patient.

Autosomal variants that likely cause ID

EP300 variant in patient 9

Mutations in *EP300* (MIM# 602700) are responsible for roughly 8% of patients with Rubinstein–Taybi syndrome (RSTS; MIM# 613684), although the clinical presentation is generally milder and typical diagnostic signs may be absent [Negri et al., 2016]. RSTS is characterized by postnatal growth retardation, microcephaly, facial dysmorphism and ID [Rusconi et al., 2015]. So far, 34 different *EP300* alterations have been identified [Negri et al., 2016]. RSTS is autosomal dominant and therefore, almost all reported mutations occurred *de novo* [Roelfsema and Peters 2007]. Patient 9 presented with a RSTS-like phenotype, for which *CREBBP* mutations were excluded previously. We detected an in-frame deletion of 12 nucleotides in *EP300*, which was not reported in either the NGS-Logistics or the EVS databases. We therefore believe this novel *EP300* variant on chromosome 22 is responsible for her ID phenotype and not a mutation on the X chromosome. We did not detect any potential cause for skewing.

SYNGAP1 variant in patient 10

Heterozygous loss-of-function *de novo* mutations in *SYNGAP1* (MIM# 603384) have been reported to cause ID (MIM# 612621). So far, 36 individuals have been described (Supp. Table S7). *SYNGAP1* mutations were initially described to be nonsyndromic but Parker and his team speculate that a clinically recognizable syndrome may be emerging [Parker et al., 2015]. Besides moderate-severe ID, other features common in *SYNGAP1* mutation carriers are language impairment, characteristic facial features, generalized hyperexcitability, sleep disturbance and an inclination to aggression [Parker et al., 2015]. In patient 10, we detected a nonsynonymous variant (p.S1165L) in *SYNGAP1* on chromosome 6. We also identified an indel over the exon-intron boundary of exon 5 in *TAF9B* (MIM# 300754), which is located on the X chromosome. *TAF9B* is a core promoter factor and regulates neuronal gene expression [Herrera et al., 2014]. This is the first report of a *TAF9B* variant -in human. Taf9b KO mice were both viable and fertile although the number of pups and their birth weights were reduced in Taf9b KO matings, compared to WT controls [Herrera et al., 2014]. No behavioral studies were performed. Therefore, the role of the *TAF9B* variant in our patient remains unclear. To

sum up, based on the available literature we hypothesize that the *SYNGAP1* variant is responsible for ID in patient 10 and we propose that the *TAF9B* variant might be responsible for skewing.

SUPP. REFERENCES

Abidi A, Mignon-Ravix C, Cacciagli P, Girard N, Milh M, Villard L. 2016. Early-onset epileptic encephalopathy as the initial clinical presentation of WDR45 deletion in a male patient. Eur J Hum Genet 24:615-618.

Ansari M, Poke G, Ferry Q, Williamson K, Aldridge R, Meynert AM, Bengani H, Chan CY, Kayserili H, Avci S, Hennekam RC, Lampe AK et al. 2014. Genetic heterogeneity in Cornelia de Lange syndrome (CdLS) and CdLS-like phenotypes with observed and predicted levels of mosaicism. J Med Genet 51:659-668.

Berryer MH, Hamdan FF, Klitten LL, Moller RS, Carmant L, Schwartzentruber J, Patry L, Dobrzeniecka S, Rochefort D, Neugnot-Cerioli M, Lacaille JC, Niu Z et al. 2013. Mutations in SYNGAP1 cause intellectual disability, autism, and a specific form of epilepsy by inducing haploinsufficiency. Hum Mutat 34:385-394.

Boyle MI, Jespersgaard C, Brondum-Nielsen K, Bisgaard AM, Tumer Z. 2015. Cornelia de Lange syndrome. Clin Genet 88:1-12.

Burdon KP, McKay JD, Sale MM, Russell-Eggitt IM, Mackey DA, Wirth MG, Elder JE, Nicoll A, Clarke MP, FitzGerald LM, Stankovich JM, Shaw MA et al. 2003. Mutations in a novel gene, NHS, cause the pleiotropic effects of Nance-Horan syndrome, including severe congenital cataract, dental anomalies, and mental retardation. Am J Hum Genet 73:1120-1130.

Callier P, Aral B, Hanna N, Lambert S, Dindy H, Ragon C, Payet M, Collod-Beroud G, Carmignac V, Delrue MA, Goizet C, Philip N et al. 2013. Systematic molecular and cytogenetic screening of 100 patients with marfanoid syndromes and intellectual disability. Clin Genet 84:507-521.

Carrel L, Willard HF. 2005. X-inactivation profile reveals extensive variability in X-linked gene expression in females. Nature 434:400-404.

Carvill GL, Heavin SB, Yendle SC, McMahon JM, O'Roak BJ, Cook J, Khan A, Dorschner MO, Weaver M, Calvert S, Malone S, Wallace G et al. 2013. Targeted resequencing in

epileptic encephalopathies identifies de novo mutations in CHD2 and SYNGAP1. Nat Genet 45:825-830.

Christodoulou J, Grimm A, Maher T, Bennetts B. 2003. RettBASE: The IRSA MECP2 variation database-a new mutation database in evolution. Hum Mutat 21:466-472.

Colvin L, Leonard H, de KN, Davis M, Weaving L, Williamson S, Christodoulou J. 2004. Refining the phenotype of common mutations in Rett syndrome. J Med Genet 41:25-30.

de Ligt J, Willemsen MH, van Bon BW, Kleefstra T, Yntema HG, Kroes T, Vulto-van Silfhout AT, Koolen DA, de Vries P, Gilissen C, del Rosario M, Hoischen A et al. 2012. Diagnostic exome sequencing in persons with severe intellectual disability. N Engl J Med 367:1921-1929.

Deardorff MA, Bando M, Nakato R, Watrin E, Itoh T, Minamino M, Saitoh K, Komata M, Katou Y, Clark D, Cole KE, De Baere E et al. 2012. HDAC8 mutations in Cornelia de Lange syndrome affect the cohesin acetylation cycle. Nature 489:313-317.

Feng L, Zhou D, Zhang Z, Liu Y, Yang Y. 2015. Exome sequencing identifies a de novo mutation in HDAC8 associated with Cornelia de Lange syndrome. J Hum Genet 60:165.

Florijn RJ, Loves W, Maillette de Buy Wenniger-Prick LJ, Mannens MM, Tijmes N, Brooks SP, Hardcastle AJ, Bergen AA. 2006. New mutations in the NHS gene in Nance-Horan Syndrome families from the Netherlands. Eur J Hum Genet 14:986-990.

Gervasini C, Russo S, Cereda A, Parenti I, Masciadri M, Azzollini J, Melis D, Aravena T, Doray B, Ferrarini A, Garavelli L, Selicorni A et al. 2013. Cornelia de Lange individuals with new and recurrent SMC1A mutations enhance delineation of mutation repertoire and phenotypic spectrum. Am J Med Genet A 161A:2909-2919.

Gilissen C, Hehir-Kwa JY, Thung DT, van de Vorst M, van Bon BW, Willemsen MH, Kwint M, Janssen IM, Hoischen A, Schenck A, Leach R, Klein R et al. 2014. Genome sequencing identifies major causes of severe intellectual disability. Nature 511:344-347.

Gonzales ML, LaSalle JM. 2010. The role of MeCP2 in brain development and neurodevelopmental disorders. Curr Psychiatry Rep 12:127-134.

Graham JM, Jr., Schwartz CE. 2013. MED12 related disorders. Am J Med Genet A 161A:2734-2740.

Graham JM, Jr., Visootsak J, Dykens E, Huddleston L, Clark RD, Jones KL, Moeschler JB, Opitz JM, Morford J, Simensen R, Rogers RC, Schwartz CE et al. 2008. Behavior of

10 patients with FG syndrome (Opitz-Kaveggia syndrome) and the p.R961W mutation in the MED12 gene. Am J Med Genet A 146A:3011-3017.

Haack TB, Hogarth P, Kruer MC, Gregory A, Wieland T, Schwarzmayr T, Graf E, Sanford L, Meyer E, Kara E, Cuno SM, Harik SI et al. 2012. Exome sequencing reveals de novo WDR45 mutations causing a phenotypically distinct, X-linked dominant form of NBIA. Am J Hum Genet 91:1144-1149.

Hamdan FF, Daoud H, Piton A, Gauthier J, Dobrzeniecka S, Krebs MO, Joober R, Lacaille JC, Nadeau A, Milunsky JM, Wang Z, Carmant L et al. 2011. De novo SYNGAP1 mutations in nonsyndromic intellectual disability and autism. Biol Psychiatry 69:898-901.

Hamdan FF, Gauthier J, Spiegelman D, Noreau A, Yang Y, Pellerin S, Dobrzeniecka S, Cote M, Perreau-Linck E, Carmant L, D'Anjou G, Fombonne E et al. 2009. Mutations in SYNGAP1 in autosomal nonsyndromic mental retardation. N Engl J Med 360:599-605.

Hamdan FF, Srour M, Capo-Chichi JM, Daoud H, Nassif C, Patry L, Massicotte C, Ambalavanan A, Spiegelman D, Diallo O, Henrion E, Dionne-Laporte A et al. 2014. De novo mutations in moderate or severe intellectual disability. PLoS Genet 10:e1004772.

Harakalova M, van den Boogaard MJ, Sinke R, van Lieshout S, van Tuil MC, Duran K, Renkens I, Terhal PA, de Kovel C, Nijman IJ, van Haelst M, Knoers NV et al. 2012. X-exome sequencing identifies a HDAC8 variant in a large pedigree with X-linked intellectual disability, truncal obesity, gynaecomastia, hypogonadism and unusual face. J Med Genet 49:539-543.

Hayflick SJ, Kruer MC, Gregory A, Haack TB, Kurian MA, Houlden HH, Anderson J, Boddaert N, Sanford L, Harik SI, Dandu VH, Nardocci N et al. 2013. beta-Propeller protein-associated neurodegeneration: a new X-linked dominant disorder with brain iron accumulation. Brain 136:1708-1717.

Herrera FJ, Yamaguchi T, Roelink H, Tjian R. 2014. Core promoter factor TAF9B regulates neuronal gene expression. Elife 3:e02559.

Hong N, Chen YH, Xie C, Xu BS, Huang H, Li X, Yang YQ, Huang YP, Deng JL, Qi M, Gu YS. 2014. Identification of a novel mutation in a Chinese family with Nance-Horan syndrome by whole exome sequencing. J Zhejiang Univ Sci B 15:727-734.

Ichinose Y, Miwa M, Onohara A, Obi K, Shindo K, Saitsu H, Matsumoto N, Takiyama Y. 2014. Characteristic MRI findings in beta-propeller protein-associated neurodegeneration (BPAN). Neurol Clin Pract 4:175-177.

Kaiser FJ, Ansari M, Braunholz D, Concepcion Gil-Rodriguez M, Decroos C, Wilde JJ, Fincher CT, Kaur M, Bando M, Amor DJ, Atwal PS, Bahlo M et al. 2014. Loss-of-function HDAC8 mutations cause a phenotypic spectrum of Cornelia de Lange syndrome-like features, ocular hypertelorism, large fontanelle and X-linked inheritance. Hum Mol Genet 23:2888-2900.

Khalifa M, Naffaa L. 2015. Exome sequencing reveals a novel WDR45 frameshift mutation and inherited POLR3A heterozygous variants in a female with a complex phenotype and mixed brain MRI findings. Eur J Med Genet 58:381-386.

Klitten LL, Moller RS, Nikanorova M, Silahtaroglu A, Hjalgrim H, Tommerup N. 2011. A balanced translocation disrupts SYNGAP1 in a patient with intellectual disability, speech impairment, and epilepsy with myoclonic absences (EMA). Epilepsia 52:e190-e193.

Krepischi AC, Rosenberg C, Costa SS, Crolla JA, Huang S, Vianna-Morgante AM. 2010. A novel de novo microdeletion spanning the SYNGAP1 gene on the short arm of chromosome 6 associated with mental retardation. Am J Med Genet A 152A:2376-2378.

Lederer D, Grisart B, Digilio MC, Benoit V, Crespin M, Ghariani SC, Maystadt I, Dallapiccola B, Verellen-Dumoulin C. 2012. Deletion of KDM6A, a histone demethylase interacting with MLL2, in three patients with Kabuki syndrome. Am J Hum Genet 90:119-124.

Lesca G, Moizard MP, Bussy G, Boggio D, Hu H, Haas SA, Ropers HH, Kalscheuer VM, des Portes V, Labalme A, Sanlaville D, Edery P et al. 2013. Clinical and neurocognitive characterization of a family with a novel MED12 gene frameshift mutation. Am J Med Genet A 161A:3063-3071.

Li A, Li B, Wu L, Yang L, Chen N, Ma Z. 2015. Identification of a novel NHS mutation in a Chinese family with Nance-Horan syndrome. Curr Eye Res 40:434-438.

Limongelli G, Russo S, Digilio MC, Masciadri M, Pacileo G, Fratta F, Martone F, Maddaloni V, D'Alessandro R, Calabro P, Russo MG, Calabro R et al. 2010. Hypertrophic cardiomyopathy in a girl with Cornelia de Lange syndrome due to mutation in SMC1A. Am J Med Genet A 152A:2127-2129.

Long M, Abdeen N, Geraghty MT, Hogarth P, Hayflick S, Venkateswaran S. 2015. Novel
        WDR45 Mutation and Pathognomonic BPAN Imaging in a Young Female With Mild
        Cognitive Delay. Pediatrics 136:e714-e717.

Lundvall M1, Samuelsson L, Kyllerman M. 2006. Male Rett phenotypes in T158M and
        R294X MeCP2-mutations. Neuropediatrics 37:296-301.

Lyons MJ, Graham JM, Jr., Neri G, Hunter AG, Clark RD, Rogers RC, Moscarda M, Boccuto
        L, Simensen R, Dodd J, Robertson S, DuPont BR et al. 2009. Clinical experience in
        the evaluation of 30 patients with a prior diagnosis of FG syndrome. J Med Genet
        46:9-13.

Negri G, Magini P, Milani D, Colapietro P, Rusconi D, Scarano E, Bonati MT, Priolo M,
        Crippa M, Mazzanti L, Wischmeijer A, Tamburrino F et al. 2016. From Whole Gene
        Deletion to Point Mutations of EP300-Positive Rubinstein-Taybi Patients: New
        Insights into the Mutational Spectrum and Peculiar Clinical Hallmarks. Hum Mutat
        37:175-183.

Nishioka K, Oyama G, Yoshino H, Li Y, Matsushima T, Takeuchi C, Mochizuki Y, Mori-
        Yoshimura M, Murata M, Yamasita C, Nakamura N, Konishi Y et al. 2015. High
        frequency of beta-propeller protein-associated neurodegeneration (BPAN) among
        patients with intellectual disability and young-onset parkinsonism. Neurobiol Aging
        36:2004-2004.

Ohba C, Nabatame S, Iijima Y, Nishiyama K, Tsurusaki Y, Nakashima M, Miyake N, Tanaka
        F, Ozono K, Saitsu H, Matsumoto N. 2014. De novo WDR45 mutation in a patient
        showing clinically Rett syndrome with childhood iron deposition in brain. J Hum
        Genet 59:292-295.

Okamoto N, Ikeda T, Hasegawa T, Yamamoto Y, Kawato K, Komoto T, Imoto I. 2014. Early
        manifestations of BPAN in a pediatric patient. Am J Med Genet A 164A:3095-3099.

Ozawa T, Koide R, Nakata Y, Saitsu H, Matsumoto N, Takahashi K, Nakano I, Orimo S.
        2014. A novel WDR45 mutation in a patient with static encephalopathy of childhood
        with neurodegeneration in adulthood (SENDA). Am J Med Genet A 164A:2388-2390.

Parenti I, Rovina D, Masciadri M, Cereda A, Azzollini J, Picinelli C, Limongelli G, Finelli P,
        Selicorni A, Russo S, Gervasini C, Larizza L. 2014. Overall and allele-specific
        expression of the SMC1A gene in female Cornelia de Lange syndrome patients and
        healthy controls. Epigenetics 9:973-979.

Parker MJ, Fryer AE, Shears DJ, Lachlan KL, McKee SA, Magee AC, Mohammed S,
        Vasudevan PC, Park SM, Benoit V, Lederer D, Maystadt I et al. 2015. De novo,

heterozygous, loss-of-function mutations in SYNGAP1 cause a syndromic form of intellectual disability. Am J Med Genet A 167:2231-2237.

Pinto D, Pagnamenta AT, Klei L, Anney R, Merico D, Regan R, Conroy J, Magalhaes TR, Correia C, Abrahams BS, Almeida J, Bacchelli E et al. 2010. Functional impact of global rare copy number variation in autism spectrum disorders. Nature 466:368-372.

Rathore GS, Schaaf CP, Stocco AJ. 2014. Novel mutation of the WDR45 gene causing beta-propeller protein-associated neurodegeneration. Mov Disord 29:574-575.

Rauch A, Wieczorek D, Graf E, Wieland T, Endele S, Schwarzmayr T, Albrecht B, Bartholdi D, Beygo J, Di Donato N, Dufke A, Cremer K et al. 2012. Range of genetic mutations associated with severe non-syndromic sporadic intellectual disability: an exome sequencing study. Lancet 380:1674-1682.

Redin C, Gerard B, Lauer J, Herenger Y, Muller J, Quartier A, Masurel-Paulet A, Willems M, Lesca G, El-Chehadeh S, Le Gras S, Vicaire S et al. 2014. Efficient strategy for the molecular diagnosis of intellectual disability using targeted high-throughput sequencing. J Med Genet 51:724-736.

Risheg H, Graham JM, Jr., Clark RD, Rogers RC, Opitz JM, Moeschler JB, Peiffer AP, May M, Joseph SM, Jones JR, Stevenson RE, Schwartz CE et al. 2007. A recurrent mutation in MED12 leading to R961W causes Opitz-Kaveggia syndrome. Nat Genet 39:451-453.

Roelfsema JH, Peters DJ. 2007. Rubinstein-Taybi syndrome: clinical and molecular overview. Expert Rev Mol Med 9:1-16.

Rump P, Niessen RC, Verbruggen KT, Brouwer OF, de Raad M, Hordijk R. 2011. A novel mutation in MED12 causes FG syndrome (Opitz-Kaveggia syndrome). Clin Genet 79:183-188.

Rusconi D, Negri G, Colapietro P, Picinelli C, Milani D, Spena S, Magnani C, Silengo MC, Sorasio L, Curtisova V, Cavaliere ML, Prontera P et al. 2015. Characterization of 14 novel deletions underlying Rubinstein-Taybi syndrome: an update of the CREBBP deletion repertoire. Hum Genet 134:613-626.

Ryu SW, Kim JS, Lee SH. 2015. Beta-Propeller-Protein-Associated Neurodegeneration: A Case of Mutation in WDR45. J Clin Neurol 11:289-291.

Saitsu H, Nishimura T, Muramatsu K, Kodera H, Kumada S, Sugai K, Kasai-Yoshida E, Sawaura N, Nishida H, Hoshino A, Ryujin F, Yoshioka S et al. 2013. De novo mutations in the autophagy gene WDR45 cause static encephalopathy of childhood with neurodegeneration in adulthood. Nat Genet 45:445-9, 449e1.

Schwartz CE, Tarpey PS, Lubs HA, Verloes A, May MM, Risheg H, Friez MJ, Futreal PA, Edkins S, Teague J, Briault S, Skinner C et al. 2007. The original Lujan syndrome family has a novel missense mutation (p.N1007S) in the MED12 gene. J Med Genet 44:472-477.

Snijders Blok L, Madsen E, Juusola J, Gilissen C, Baralle D, Reijnders MR, Venselaar H, Helsmoortel C, Cho MT, Hoischen A, Vissers LE, Koemans TS et al. 2015. Mutations in DDX3X Are a Common Cause of Unexplained Intellectual Disability with Gender-Specific Effects on Wnt Signaling. Am J Hum Genet 97:343-352.

Takano K, Shiba N, Wakui K, Yamaguchi T, Aida N, Inaba Y, Fukushima Y, Kosho T. 2016. Elevation of neuron specific enolase and brain iron deposition on susceptibility-weighted imaging as diagnostic clues for beta-propeller protein-associated neurodegeneration in early childhood: Additional case report and review of the literature. Am J Med Genet A 170:322-328.

Tschentscher A, Dekomien G, Ross S, Cremer K, Kukuk GM, Epplen JT, Hoffjan S. 2015. Analysis of the C19orf12 and WDR45 genes in patients with neurodegeneration with brain iron accumulation. J Neurol Sci 349:105-109.

Tug E, Dilek NF, Javadiyan S, Burdon KP, Percin FE. 2013. A Turkish family with Nance-Horan Syndrome due to a novel mutation. Gene 525:141-145.

Tzschach A, Grasshoff U, Beck-Woedl S, Dufke C, Bauer C, Kehrer M, Evers C, Moog U, Oehl-Jaschkowitz B, Di Donato N, Maiwald R, Jung C et al. 2015. Next-generation sequencing in X-linked intellectual disability. Eur J Hum Genet 23:1513-1518.

Van Goethem G, Livingston JH, Warren D, Oojageer AJ, Rice GI, Crow YJ. 2014. Basal ganglia calcification in a patient with beta-propeller protein-associated neurodegeneration. Pediatr Neurol 51:843-845.

Verhoeven WM, Egger JI, Koolen DA, Yntema H, Olgiati S, Breedveld GJ, Bonifati V, van de Warrenburg BP. 2014. Beta-propeller protein-associated neurodegeneration (BPAN), a rare form of NBIA: novel mutations and neuropsychiatric phenotype in three adult patients. Parkinsonism Relat Disord 20:332-336.

Vissers LE, de Ligt J, Gilissen C, Janssen I, Steehouwer M, de Vries P, van Lier B, Arts P, Wieskamp N, del Rosario M, van Bon BW, Hoischen A et al. 2010. A de novo paradigm for mental retardation. Nat Genet 42:1109-1112.

Vulto-van Silfhout AT, de Vries BB, van Bon BW, Hoischen A, Ruiterkamp-Versteeg M, Gilissen C, Gao F, van ZM, Harteveld CL, van Essen AJ, Hamel BC, Kleefstra T et al.

2013. Mutations in MED12 cause X-linked Ohdo syndrome. Am J Hum Genet 92:401-406.

Walpole IR, Hockey A, Nicoll A. 1990. The Nance-Horan syndrome. J Med Genet 27:632-634.

Writzl K, Knegt AC. 2013. 6p21.3 microdeletion involving the SYNGAP1 gene in a patient with intellectual disability, seizures, and severe speech impairment. Am J Med Genet A 161A:1682-1685.

Zollino M, Gurrieri F, Orteschi D, Marangi G, Leuzzi V, Neri G. 2011. Integrated analysis of clinical signs and literature data for the diagnosis and therapy of a previously undescribed 6p21.3 deletion syndrome. Eur J Hum Genet 19:239-242.